Photonics Innovation Hub

APPLICATION NOTE - #AN-2601

# MICROSPHERE FABRICATION USING A CO2 LASER GLASS PROCESSING STATION

*K. Terrien, A. Haboucha, B. Dudoux*

## Scope and Overview:

Photonics Bretagne is equipped with a vertical glass processing station, the *SmartSplicer™* from *Nyfors*. The heat source of the station is a CO2 laser that emits at a wavelength of 10.6µm. The CO2 laser was selected by the manufacturer of the station, as silica exhibits a pronounced absorption at 10.6µm [4]. This facilitates the rapid and extensive heating of the fiber.

The ring-shaped laser beam of the station is particularly well-suited to the fabrication of optical fiber-based components, due to the uniform distribution of heat around the fiber and especially microspheres.

Microspheres have a variety of applications, including ball lenses for optimising fiber coupling [1], sensors [2], micro-cavities or high-Q whispering-gallery-mode micro-resonators [3].

## Microsphere Design:

Microsphere design is contingent on volume conservation, as asserted by [1]. This means that the radius of the desired sphere is determined by the volume of matter utilised to fabricate it.

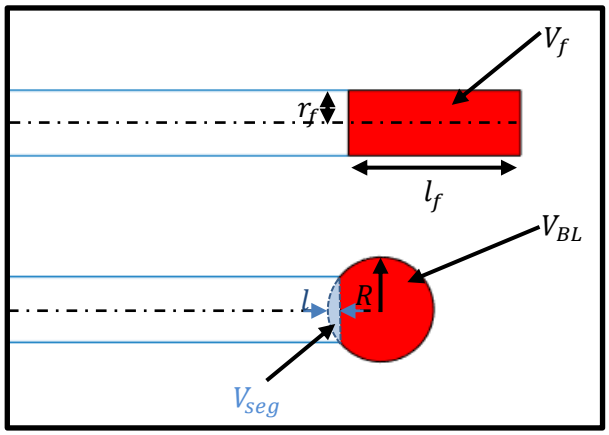


*Fig. 1 - Schematic representation of the microsphere design*

The volume of the initial fiber $V_f$ is defined as:

$$V_f = V_{BL} - V_{seg} \qquad (1)$$

Here $V_{BL}$ is the volume of the ball lens to fabricate and $V_{seg}$ the volume of the imaginary segment defined as the cross section of the ball-lens and the fiber.

The length of this segment is given by:

$$l = R - \sqrt{R^2 - r_f^2} \qquad (2)$$

In equation (2), R and $r_f$ are respectively the radius of the ball-lens fabricated and the radius of the initial fiber.

The different volumes can be expressed easily:

$$\begin{cases} V_f = \pi r_f^2 l_f \\ V_{BL} = \frac{4}{3}\pi R^3 \\ V_{seg} = \frac{\pi}{3} l^2 \times (3R - l) \end{cases} \qquad (3)$$

The initial length of fiber required to create a ball lens with a radius of R can be determined by rearranging equation (1) with equations (3):

$$l_f = \frac{1}{\pi r_f^2} \times \left(\frac{4}{3}\pi R^3 - V_{seg}\right) \qquad (4)$$

The target diameters are 100µm, 160µm and 250µm. Given that the fiber diameter is 125µm, the initial fiber lengths required for the 160µm and 250µm microspheres must be 153µm and 655µm, respectively.

Microspheres with an outer diameter of 100µm require to taper the fiber prior realizing the microsphere.

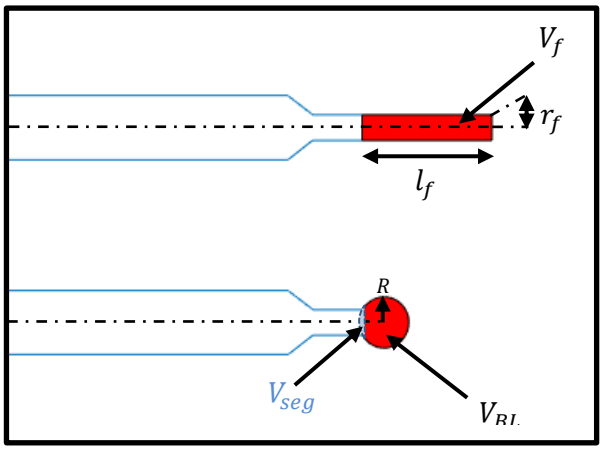


*Fig. 2 - Schematic representation of the microsphere design on a taperised fiber*

The waist diameter of the tapered fiber is fixed to 50µm to empathize the roundness of the microsphere. The diameter of the initial fiber is considered as 50µm and then the length of initial fiber required to manufacture a 100µm diameter microsphere is around 260µm.

## *CO2 station configuration:*

The station offers two main configurations for the beam shape. The first is the end-cap type configuration (cf. Fig. 3(a)), and the second is the taper type configuration (cf. Fig. 3(b)).

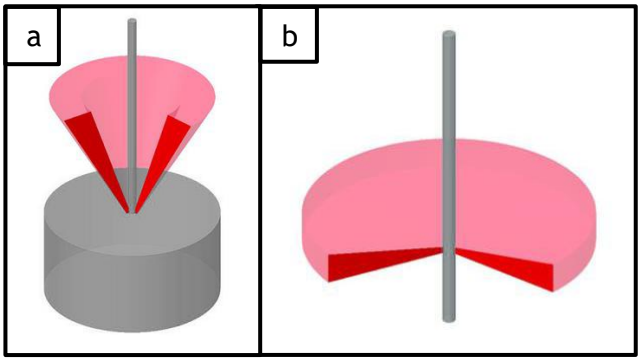


*Fig. 3 - The laser shape is set depending on the component to manufacture [8] - picture credit: Nyfors*

In order to realise the microsphere, it is necessary to set the station in the taper type configuration.

As previously mentioned, it may also be advisable to consider the implementation of a taper prior to the microsphere, with a view to achieving enhanced roundness.

Regarding the different target diameters, the fiber is tapered for microspheres of 100µm diameter but not for the ones with 160 and 250µm diameter.

As a vertical station, the *SmartSplicer™* enables the cleaved end of the fiber to be oriented in either a face-down or face-up configuration.

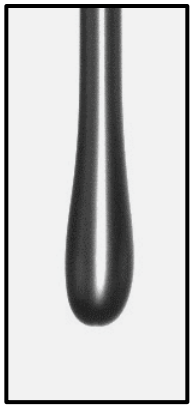

*Fig. 4 - Microsphere realized using the upper holder - picture credit: Nyfors*

It is evident that both methods are viable options. However, orienting the fiber such that its cleaved end faces downwards may result in the microsphere undergoing an elongation during the process.

This is attributed to the gravitational forces at play, which can potentially lead to a sphere that deviates from a perfect spherical shape. *Figure 4* illustrates this effect, showing a microsphere fabricated using the upper holder, where gravitational stretching led to a noticeable deviation from perfect roundness.

In order to foster the roundness of the microsphere during the heating of the fiber, it is advantageous to use the lower holder, taking advantage of gravity.

By solving the equation described below [5-7]:

$$\rho C_p - \nabla \cdot (k \nabla T) = Q \qquad (5)$$

where T is the temperature, ρ is the density, $C_p$ is the heat capacity, k is the thermal conductivity and Q is the heat source term, the evolution of the temperature at the surface of the fiber can be estimated for different power settings.

The Fig. 5 shows that the temperature at the surface of the fiber increases rapidly, depending on the laser power setting. In some cases, it can even exceed the vaporization point of fused silica (~2700°C), which is consistent with observations.

The laser power is set to approximately 2% of its maximum value, ensuring that the fiber reaches a temperature sufficient for gentle melting.

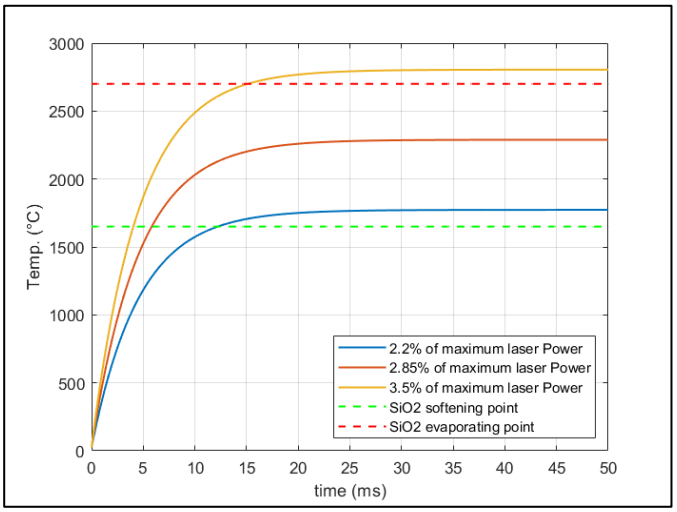


*Fig. 5 - Temperature evolution depending on the laser power*

## *Microspheres Fabrication:*

The fiber is subsequently introduced into the station, and the displacement length is adjusted according to the target diameter (see “Microspheres Design” chapter).

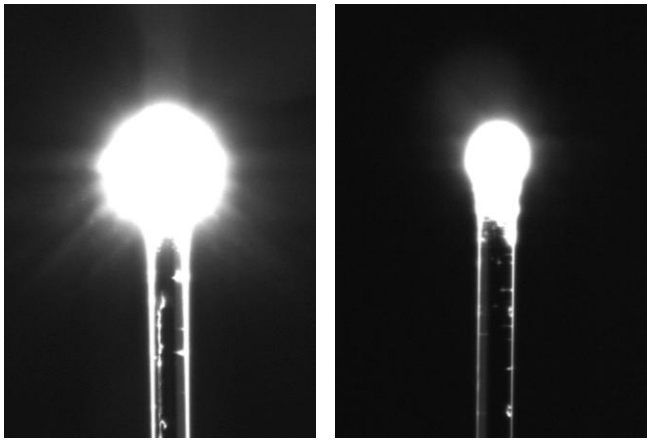

*Fig. 6 - The fiber during the ball growing step (left) and during the rounding process (right)*

In Figure 6, the left side shows the fiber during the formation of the microsphere under laser heating. The right side captures the rounding phase, which follows immediately after and is essential for stabilizing the final shape.

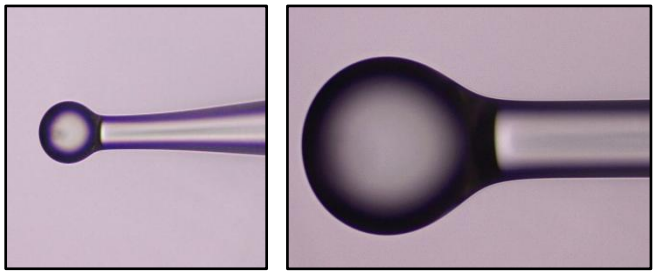

*Fig. 7 - Optical microscope images of microspheres with diameters of 100µm (left) and 250µm (right), observed using the Leica DM750M microscope.*

The resultant microspheres are then observed and characterized with an optical microscope. As illustrated in *Figure 7*, microspheres with diameters of 100µm (left) and 250µm (right) were successfully produced and imaged using the Leica DM750M microscope.

## *References:*


[1] Brueckner, H. J., Chai, L. Y., Tiedeken, S., Braun, V., & Teubner, U. (2023). Design considerations and experimental investigations on fiber ball lens systems for optical metrology. *Journal of Physics Photonics*, *5*(3), 035004. https://doi.org/10.1088/2515-7647/acdba6

[2] Shaimerdenova, M., Ayupova, T., Sypabekova, M., & Tosi, D. (2020). Fiber optic refractive index sensors based on a ball resonator and optical backscatter interrogation. *Sensors*, *20*(21), 6199. https://doi.org/10.3390/s20216199

[3] Perin, G., Dumeige, Y., Féron, P., & Trebaol, S. (n.d.). High-Q Whispering-Gallery-Modes microresonators in the Near-Ultraviolet Spectral range. *arXiv (Cornell University)*. https://doi.org/10.48550/arxiv.2211.03391

[4] Gallais, L., & Cormont, P. (2022). Procédés d'usinage laser CO2 de composants optiques en silice. *Photoniques*, *112*, 32–36. https://doi.org/10.1051/photon/202211232

[5] Khotiaintsev, S., & Castro-Martinez, A. (2011). Thermal treatment of silica optical fibers with CO2-laser radiation. *Electronics and Communications*, *16*(4), 172–176. https://doi.org/10.20535/2312-1807.2011.16.4.246655

[6] Tan, C., Zhao, L., Chen, M., Cheng, J., Zhang, Y., Zhang, J., & Yan, Z. (2022). Heat accumulation effect during CO2 laser processing of fused silica optics. *Results in Physics*, *34*, 105308. https://doi.org/10.1016/j.rinp.2022.105308

[7] Doualle, T., Gallais, L., Cormont, P., Hébert, D., Combis, P., & Rullier, J. (2016). Thermo-mechanical simulations of CO2 laser-fused silica interactions. *Journal of Applied Physics*, *119*(11). https://doi.org/10.1063/1.4944435

[8] SMARTSPLICER - User Manual, v13, Nyfors Teknologi AB, Stockholm, Sweden, 2024, pp. 16